



## Reactive red 198 dye removal from textile wastewater by SBA-15 modified with cationic surfactant

Siavash Afrashteh<sup>1,\*</sup>

<sup>1</sup>Department of Textile Engineering, Qaemshahr Branch, Islamic Azad University, Qaemshahr, Iran

### ARTICLE INFO

#### Article history:

Received 11 March 2024

Received in revised form 25 April 2024

Accepted 11 May 2024

Available online 4 December 2024

#### Keywords:

SBA-15, R.R. 198 removal, textile wastewater, DOTAC surfactant.

### ABSTRACT

Highly sensitive, accurate and relatively fast technique has been utilized to remove reactive red 198 (R.R. 198) dye in textile wastewater, using synthesised nanocomposites. Determination of R.R. 198 dye was carried out by UV-Vis spectrophotometer at  $\lambda_{\max}$  = 515 nm. A SBA-15 mesoporous silica was synthesized then was functionalised using dodecyl trimethyl ammonium chloride (DOTAC) cationic surfactant. TEM, elemental analysis CHNS, TGA, FT-IR, and BET techniques were used to characterize the nanocomposites features. This research studies the impact of various parameters in removal of R.R. 198 dye by nanocomposite, like pH, quantity of nanocomposite, contact time, type of eluting solvent, and concentration of R.R. 198 dye was investigated. Experiments show that the new nanocomposite (DOTAC/SBA-15) is an excellent and powerful nanocomposite for removing the R.R. 198 dye from textile wastewater such as, Mazandaran textile factory, Qaemshahr sangtab textile factory, Amol babakan textile factory and Behshahr Acryltab factory with suitable fallouts.

### 1. Introduction

Generally, scientists has encountered the challenge of contamination of natural waters caused by dyes and some noxious elements currently [1]. These harmful and venomous materials cause several serious problems in animals, human, and plants. Hence, industrial factories and chemical waste water has been emphasized in this regard [2, 3]. For example, they become unsuitable for public consumption owing to the discharged from textile dyeing mills in the natural waters [4]. There is a huge deal of highly concentrated dyes in waste water of dyeing units of a textile plant [5]. Dyes have high usage in different industries like dyestuffs, textiles, cosmetics, and paper [2, 3]. Azoic dyes as complex aromatic structures have higher resistance to biodegradation [6]. The reactive red 198 as a water-soluble azo dye is difficult to remove from wastewater. Several approaches are used to remove dyes and other color pollutants such as chemical coagulation, aerobic/anaerobic biological degradation, membrane filtration, flocculation, chemical oxidation, and photochemical degradation. Such approaches are

expensive and occasionally can not remove dyes from waste water totally [7–10]. Adsorption has been recently popular as a result of its low running costs and easy operations [11,12]. Comparing the stated method with other removal approaches, the main factors included in the higher efficiency of the adsorption method were economic justification, cost-effectiveness, and simplicity of operation. An adsorbent is involved in the adsorption method, which must be at least high effective and include proper functional groups. Thus, pollutants are removed by researchers through various adsorbents with these two features. Several adsorbents have been developed to purify wastewater including SBA-15 [13-18], CdO nanoparticles [19], multi-walled carbon nanotube [20-22], fullerene [23, 24], SDS-coated alumina [25], glass foam [26], cellulose nanofibers [27-30], copper nanowire/Carbon paste electrode [31], MgO nanoparticles [32], nickel oxide nanostructures [33], Fe<sub>3</sub>O<sub>4</sub> magnetic nanocomposite [34-37] and graphene oxide [38, 39]. Presently, a huge deal of attention has been attracted toward mesoporous materials because of their great

\* Corresponding author; e-mail: [siavash.afraشته@gmail.com](mailto:siavash.afraشته@gmail.com)

<https://doi.org/10.22034/crl.2024.4479390.1310>



This work is licensed under Creative Commons license CC-BY 4.0

practical potentials and scientific importance in catalysis, adsorbents, host materials, and sensors [40-43]. Moreover, compared to the other silica materials, the maximum hydrothermal stability is displayed by SBA-15 [44,45] that is suitable for aqueous media applications. SBA-15 functionalized with various function groups are highly utilized as adsorbent because of their higher selectivity for ions adsorption [46]. Carboxylic acid [47], iminoacetate [48], sulfonic acid [49], amino-carboxyl [50], ionic liquid [51], dispersive liquid-liquid [52], dithizone [53], and thio and amine [54] were immobilized onto various substrates for removal of dyes. In this work, a colloidal solution was prepared for the first time, based on dodecyl trimethyl ammonium chloride (DOTAC) cationic surfactant functionalized SBA-15 nanoparticles to remove reactive red 198 dye from wastewater samples via spectrophotometer. The nanoparticles structure was characterized through various methods like transmission electron microscope (TEM), Elemental analysis CHN, Emmett, Brunauer, and Teller (BET), FT-IR, and thermogravimetric analysis (TGA). The effect of various variables was then investigated such as amount of adsorbent, pH, and removal time, on the removal of reactive red 198 dye.

## 2. Materials and Methods

### 2-1. Reagents and Instruments

All chemicals were in analytical grade reagents. The solutions were made utilizing double distilled water. The anionic dye (Reactive red 198) was bought from Dystar (Fig. 1), and utilized with no further purification. A stock reactive red solution ( $1000 \text{ mg L}^{-1}$ ) was made and diluted suitably to the considered initial concentration. The dye represents a strong absorption peak at 515 nm in the visible region. This wavelength is equivalent to the highest absorption peak of the R.R. 198 ( $\lambda_{\text{max}}=515$ ). DOTAC cationic surfactant and Plaronic P-123 bought from Sigma Aldrich. To measure the pH, a Metrohm pH meter (model 744) was used with a mixed pH glass electrode calibrated against two standard buffer solutions (4.0 and 7.0). Other instruments included Trans-mission electron microscope (TEM) with specification (HitachiHigh-Technologies Europe GmbH, HF2000, Germany, 100 kV volt-age), Brunauer-Emmett-Teller technique (BET) (Quanta chrome, Chem BET 300 TPR/TPD), analysis CHNS (Costech ECS4010), thermogravimetric analysis (TGA) (Bahr thermo analyse), Fourier transform infrared (FT-IR) (Agilent Resolutions pro), and UV-Vis spectrophotometer (Jenway model 6505).

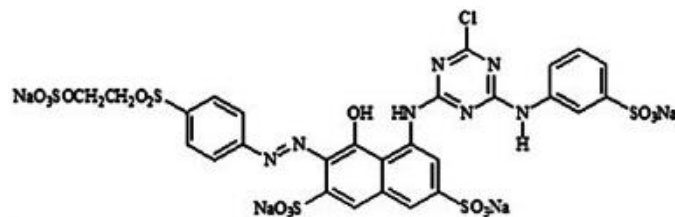


Fig. 1. The reactive red 198 chemical structure

### 2-2. Synthesis of SBA-15 mesoporous silica

SBA-15 was synthesized via a known process using a combination of triblock copolymer, Pluronic P123, HCl, TEOS, H<sub>2</sub>O, and KCl. Approximately P123 was dissolved in a combination of distilled water and HCl by adding KCl. Then, TEOS was inserted into the solution. For 24 h, the mixture was statically. The solid was recovered by filtration and rinsed with water. Then, by refluxing the surfactant was extracted via a Soxhlet extractor. The gained SBA-15 was dried at 100°C overnight[39].

### 2-3. Modification of SBA-15 nanoparticles

2.0 g of SBA-15 was inserted to NaHCO<sub>3</sub> 0.16 M (25 mL) and in into a beaker (100 mL). Then the solution was stirred for 30 min via a shaker to mix the SBA-15 with NaHCO<sub>3</sub>. The solution was centrifuged for 10 min at 5000 rpm. The SBA-15 was washed using distilled water two times by upper solution overflow at the bottom. The mixture was placed into centrifuge tube adding DOTAC cationic surfactant (1.0 g) to 50 mL acetone in a container, while stirring for 180 min via a shaker. It was centrifuged for 20 min. The centrifuging tube was placed in an oven at 60 °C based on tube overflow upper solution for drying and making powder (Fig. 2).

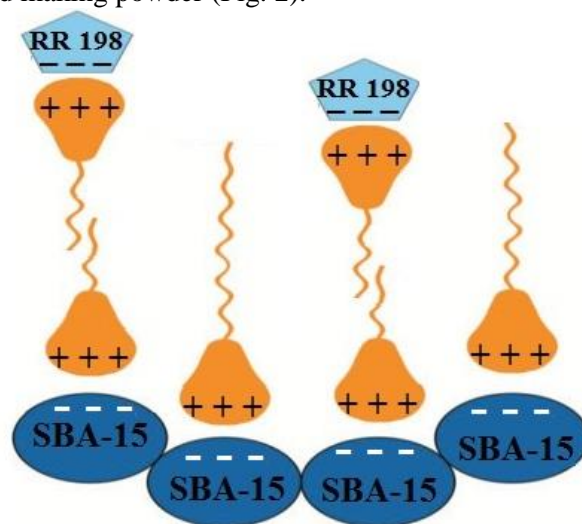


Fig. 2. A suggested binding mode of DOTAC to SBA-15 nanoparticles surface.

## 2-4. Procedure for removal of R.R. 198 dye

Firstly, 100 mL R.R. 198 solution (200 mg L<sup>-1</sup>) was created in pH=5 modified with CH<sub>3</sub>COOH/ CH<sub>3</sub>COONa buffer solution. Next, we inserted 150 mg nanocomposites to the solution (100 mL), and mixed for 20 min at ambient temperature. Ultimately, for phase separation, the product was centrifuged (at 5000 rpm for 5 min). Overflowing the upper solution, R.R. 198 dye adsorbed on the precipitation was diffused via the sample elution with 10.0 mL acetone. After mixing acetone, for 5 min the product was stirred and centrifuged again (at 5000 rpm for 10 min). Finally, spectrophotometry technique was utilized to determine R.R. 198 concentration. To optimize the best circumstances for R.R. 198 pre-concentration, various parameters were investigated such as type of eluting solvent, the nanocomposite dosage, the shaking time, and pH, so that a satisfactory removal can be achieved. In all optimization processes, R.R. 198 concentration were set as 200 mg L<sup>-1</sup>.

## 3. Results and Discussion

### 3.1. Characterizing the SBA-15 and nanocomposite

The synthesis of the SBA-15 and DOTAC functionalized SBA-15 were characterized by TEM, TGA, CHNS and BET.

Based on the TEM image (Fig. 3a), the SBA-15 pore size is < 20 nm with uniformly hexagonal structure. Fig. 3b shows the structure of SBA-15/DOTAC structure. It can be concluded from Fig. 3b that DOTAC covered the surface of SBA-15.

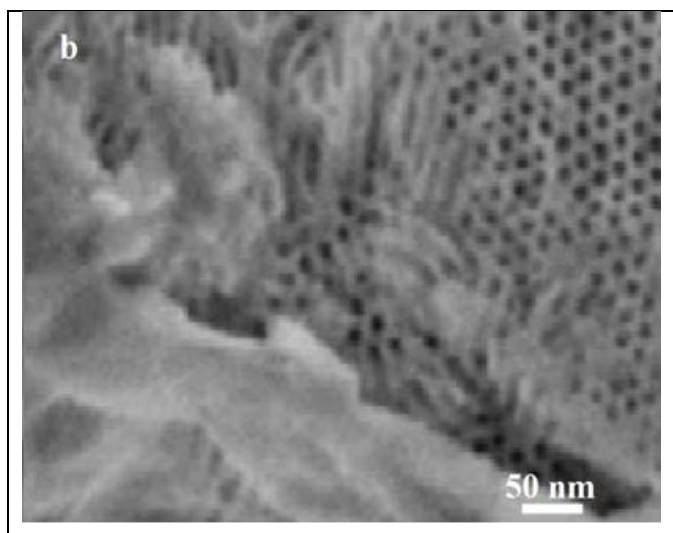
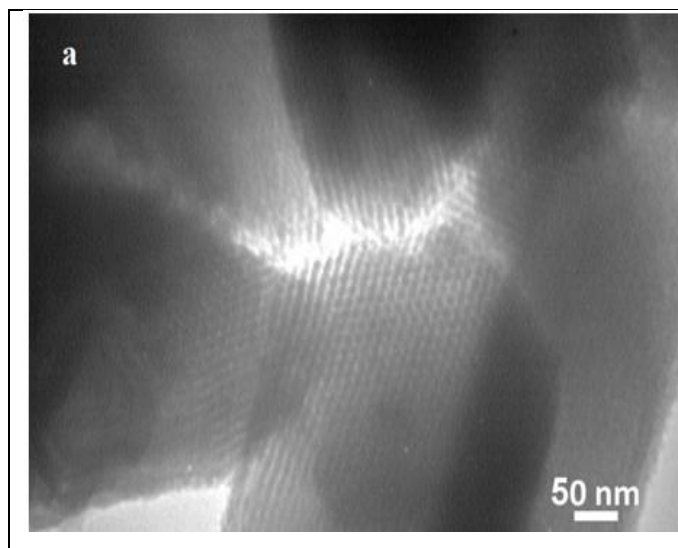


Fig. 3. (a)TEM image of the SBA-15; (b) DOTAC/SBA-15 (b)

The nanocomposites was thermogravimetrically studied to display the nanocomposite stability and the existence of organic groups in the material (Fig. 4). The weight loss 11.7% at about 120 °C in the SBA-15 (Fig. 4.a) and the mass loss (19.21%) within 245-340 °C in the nanocomposites (Fig. 4.b) are caused by the existing water and DOTAC cationic surfactant, respectively. At T > 400 °C, a small and continuous weight loss is found associated with the residual organic material combustion.

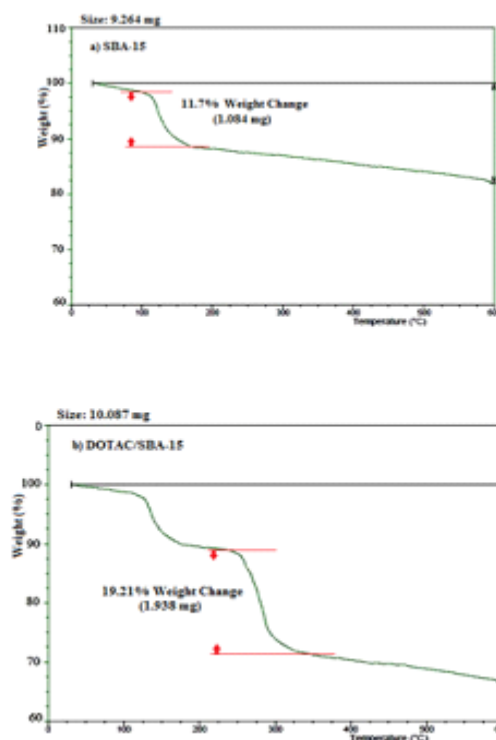


Fig. 4. TGA analysis curve for SBA-15 (a) and DOTAC/SBA-15 (b)

Through elemental analysis CHNS, the elements types were determined in synthesized nanocomposite and determination of the elements ratio in the sample. Table 1 shows the practical values of nanocomposite elements. As seen, the existence of carbon and nitrogen in CHNS analysis of nanocomposite proves the existence of DOTAC on the SBA-15 surface.

**Table 1.** The results of multi-elemental CHNS analysis on DOTAC/SBA-15

Reten. time (min)	Response	Weight (g)	Weight (%)	Element name	Carbon response ratio
2.319	2864.3	0.051	14.21	Carbon	1.000
1.395	210.6	0.005	1.39	Nitrogen	0.074
7.864	547.6	0.010	2.79	Hydrogen	1.191
16.375	0.04	0.000	0.00	Sulfur	0.000
Sample weight:		0.066	18.39		
0.359 (g)					

Measurement of the specific surface area in SBA-15 and SBA-15/DOTAC was performed by the use of the nitrogen adsorption and desorption isotherms along with the BJH method, as observed in Table 2. The hysteresis loop became wider in SBA-15/DOTAC following the loading of DOTAC, and the curved isotherm section was transferred to lower pressure, the hysteresis loop end of which was close to  $P/P_0 = 0.4$ , showing the placement of DOTAC inside SBA-15 cavities (Fig. 5). Moreover, a reduction in the specific surface area of SBA-15/DOTAC cavities was indicative of the proper placement of DOTAC particles inside the SBA-15 cavities and channels.

Furthermore, the curved isotherm section was transferred to lower  $P/P_0$  in SBA-15/DOTAC nanocomposite following surface modification and placement of DOTAC on the SBA-15 surface. This indicated the placement of DOTAC within the SBA-15 channels.

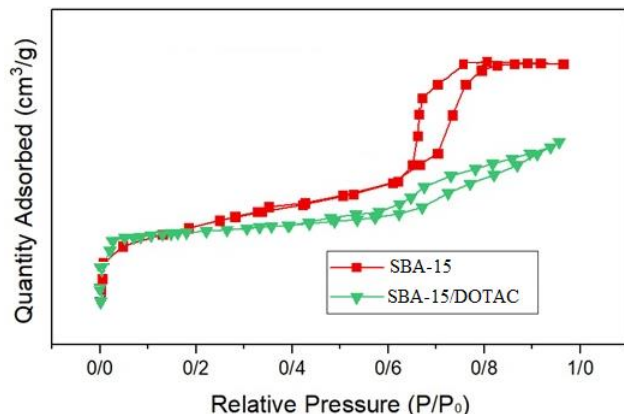


**Fig. 5.** N adsorption and desorption for SBA-15 and SBA-15/DOTAC samples.

The BET analysis on SBA-15 proved the SBA-15's specific surface area as 273.46 m<sup>2</sup>/g, which was decreased to 251.28 m<sup>2</sup>/g after surface modification. This surface dropping is predicted owing to the surface coverage by DOTAC cationic surfactant. Indeed, these two wide surfaces present good areas for R.R. 198 dye absorbance.

**Table 2.** BET analysis results from DOTAC/SBA-15

Surface area before coating (m <sup>2</sup> /g)	273.46
Surface area after coating (m <sup>2</sup> /g)	251.28
Adsorption average pore width (nm)	9.07

FT-IR was used to confirm the presence of DOTAC surfactant on SBA-15 (Figure 6). The broad absorption band at 3431 cm<sup>-1</sup> is related to the stretching vibration of the OH groups on the surface of SBA-15. Absorption band at 2923 cm<sup>-1</sup> is assigned to the stretching vibration of CH bond. The absorption band at 1450 cm<sup>-1</sup> is assigned to corresponds to the vibration of the C-H bond of the CH<sub>3</sub> group. The absorption band at 1088 cm<sup>-1</sup> corresponds to the Si-O bond of SBA-15 and it covers the absorption band related to the C-N bond of the DOTAC surfactant, which gives a spectrum in the range of 1200 cm<sup>-1</sup>.

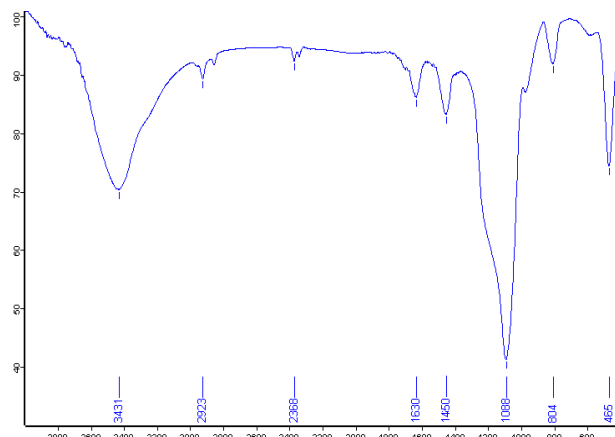


**Fig. 6.** FT-IR spectrum of SBA-15/DOTAC nanocomposite

### 3-1. Optimization of the removal stage

The effect of all the parameters affecting the removal performance should be assessed including the shaking time, type of eluting solvent, the nanocomposite dosage, pH and concentration of R.R. 198 to obtain a higher removal.

### 3-2. The effect of pH

Generally, pH is important in the adsorption process in surface adsorption load, and various adsorbent pollutants in solution, separation of different functional groups over active adsorbent sites, and the R.R. 198 dye molecule

structure. In the present work, the pH effect on the adsorption procedure of R.R. 198 dye was evaluated in the range of 3–11 by addition of NaOH or HCl for adsorbent particles (DOTAC/SBA-15 composite). As seen in Fig. 7, the pH of 5.0 was chosen for the removal of R.R. 198 dye. At the alkaline pH values, the removal percentage is low, because hydroxide ions compete with reactive red 198 dye to adsorption with the DOTAC cationic surfactant.

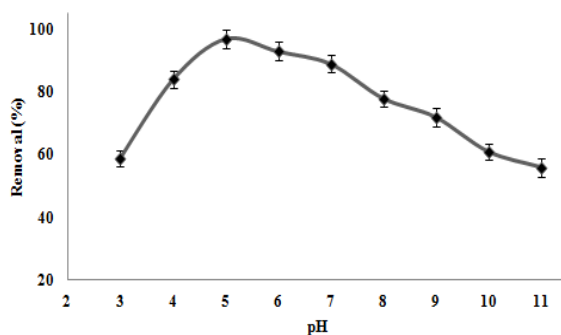


**Fig. 7.** The effects of pH on the removal. Removal conditions: Amount of sorbent, 150 mg; recovery solvent, 10.0 mL acetone; contact time, 20 min; R.R. 198 concentration, 200 mg L<sup>-1</sup>.

### 3-3. Impact of the nanocomposite dosage

The effect of different quantities of sorbent (modified SBA-15) on the removal of R.R. 198 dye were assessed within 50–200 mg range. It is indicated (Fig. 8) that R.R. 198 dye was adsorbed completely on the sorbent in the 150 mg of the modified SBA-15. Thus, 150 mg was chosen as the sorbent essential for all subsequent tests.

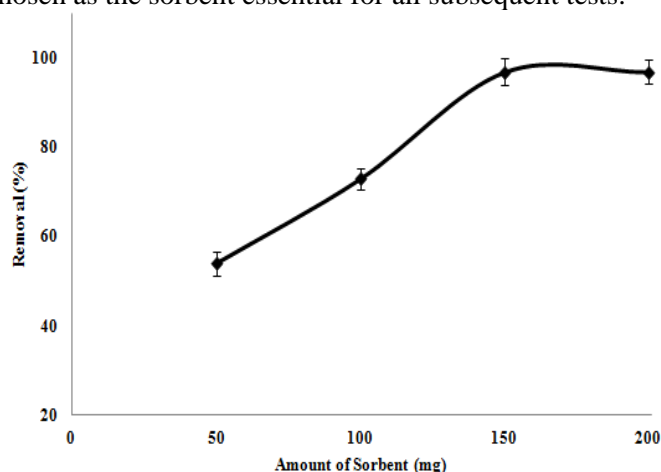


**Fig. 8.** Effects of nanosorbent amount on the removal. Removal circumstances: pH value, 5.0; recovery solvent, 10.0 mL acetone; contact time, 20 min; R.R. 198 concentration, 200 mg L<sup>-1</sup>.

### 3-4. Impact of contact time

The removal of the R.R. 198 dye is based on the sample contact time with the solid phase. Therefore, repeated sets of adsorbents and dye were made to assess at different time intervals (5, 10, 15, 20, 25 and 30 min). It was revealed that the rate of dye uptake was higher (Fig. 9). At about 20 min, the of dye adsorption from the solution was over 96%.

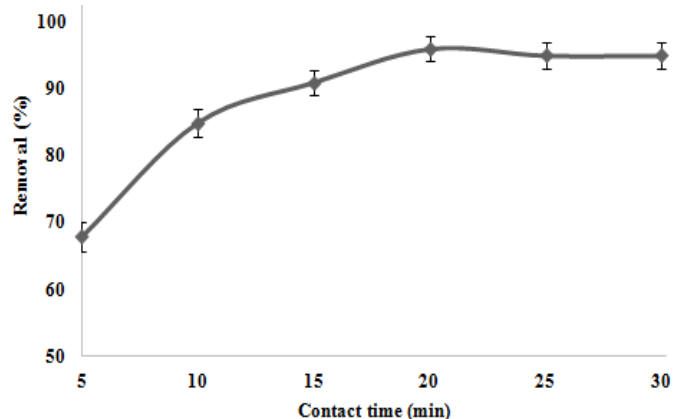


**Fig. 9.** The kinetics of dye adsorption on modified SBA-15. Removal conditions: Amount of sorbent, 150 mg; pH value, 5.0; recovery solvent, 10.0 mL acetone; R.R. 198 concentration, 200 mg L<sup>-1</sup>.

### 3-5. The effect of type of eluting solvent

Different tests were conducted to achieve optimum conditions for total elution of R.R. 198 dye on DOTAC/SBA-15. We exerted 10.0 mL of different solvent types as the optimum eluent for future experiments. According to Fig. 10, acetone provides the most optimum quantitative elution of R.R. 198 dye mixed with DOTAC/SBA-15.

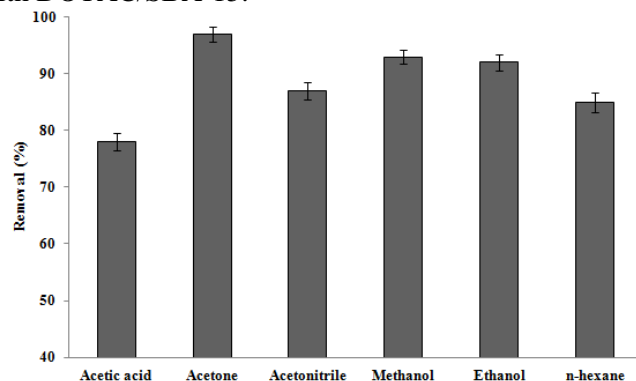


**Fig. 10.** The effect of type of eluent on the removal of R.R. 198 dye. Removal conditions: Amount of sorbent, 150 mg; pH value, 5.0; contact time, 20 min; R.R. 198 concentration, 200 mg L<sup>-1</sup>.

### 3-6. Effect of R.R. 198 concentration

To investigate the possibility of our presented sorbent with respect to various R.R. 198 concentrations, the

effects of various concentrations of this dye were investigated within the range of 50 to 300 mg L<sup>-1</sup>. A higher adsorption value was found at the lower concentration of R.R. 198. However, by increasing the dye dosage to 250 mg L<sup>-1</sup>, the sorbent activity reduced. As seen in Fig. 11, the most suitable concentration value for R.R. 198 was 200 mg L<sup>-1</sup> in terms of the removal percent as well as the loading for the sorbent is 0.135 mmol g<sup>-1</sup>.

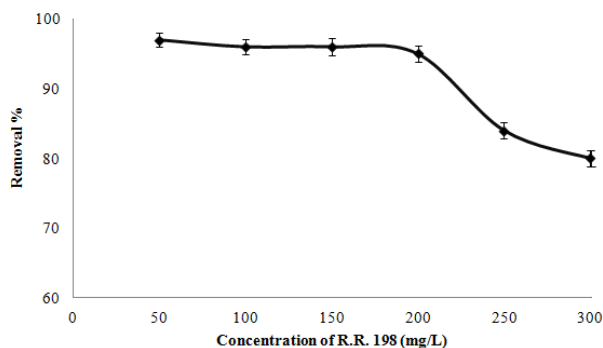


**Fig. 11.** The impacts of dye concentration on the removal. Removal conditions: Amount of sorbent, 150 mg; pH value, 5.0; contact time, 20 min; recovery solvent, 10.0 mL acetone.

### 3-7. Nanocomposite reusability

An adsorbent reusability is as a key factor in analytical approaches. As seen in Fig. 12, the reusability results for DOTAC/SBA-15, the nanocomposite can be reused for three times by rising via recovery solvent. Moreover, after three times, the adsorption level reduced to 92.5% from 96.8%. The removal reduced owing to release of the surfactant grafts, irreversible/strong interactions between surfactant and R.R. 198 dye, and nanocomposite particles loss during elution.

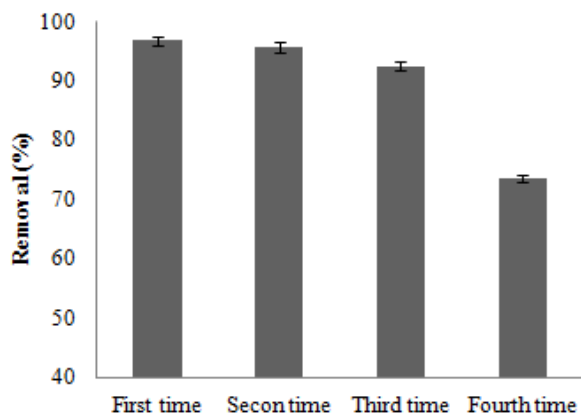


**Fig. 12.** The nanocomposite reusability. Removal conditions: Amount of sorbent, 150 mg; pH value, 5.0; contact time, 20 min; recovery solvent, 10.0 mL acetone; R.R. 198 concentration, 200 mg L<sup>-1</sup>.

### 3-8. Removing of R.R. 198 dye from textile wastewater samples

First, some textile wastewater samples (100 mL) were prepared (Table 3), and filtered via a membrane filter with a pore size of 0.45- $\mu$ m prior to any analysis for removal of any suspended particles. Furthermore, after filtration, the real concentration of R.R. 198 in textile wastewater specimens was determined by UV-Vis spectrophotometer. The higher removal percent is obtained (Table 3), for each real sample, indicating the successful use of the proposed method in removal of R.R. 198 dye in textile wastewater samples.

**Table 3.** Removal of R.R. 198 dye from textile wastewater samples

wastewater Sample	Physical-chemical information of sample	concentration of R.R. 198 (mg L <sup>-1</sup> )	Removal (%)
Mazandaran textile factory (Qaemshahr)	pH = 6.9, TSS = 127, TDS = 814, BOD = 240, COD = 360	21.21 $\pm$ 0.19	96.4 $\pm$ 1.9
Sangtab textile factory (Qaemshahr)	pH = 7.8, TSS = 136, TDS = 940, BOD = 260, COD = 390	17.63 $\pm$ 0.15	95.3 $\pm$ 2.1
Babakan textile factory (Amol)	pH = 7.3, TSS = 125, TDS = 850, BOD = 220, COD = 330	20.15 $\pm$ 0.17	97.9 $\pm$ 1.8
Acryltab factory (Behshahr)	pH = 6.6, TSS = 143, TDS = 920, BOD = 250, COD = 310	14.24 $\pm$ 0.11	95.8 $\pm$ 1.7

## 4. Conclusion

A novel operative nanosorbent was synthesized by functionalization of the SBA-15. According to the experiments, the new modified SBA-15 with DOTAC cationic surfactant is a strong sorbent for removing the R.R. 198 dye from textile wastewater. This method indicates that removal more than 95% R.R. 198 dye is possible at optimal conditions of pH = 5, R.R. 198 concentration = 200 mg L<sup>-1</sup>, and the sorbent dosage = 150 mg. It was indicated that, DOTAC/SBA-15 is a superior absorbent for moderate concentrations of R.R. 198. An eco-friendly non-toxic absorbent is used in the proposed method not threatening the human health. Moreover, it is highly sensitive, simple, and relatively quick.

## Acknowledgement

The author thank the Research Council at the Qaemshahr Branch, Islamic Azad University for technical and financial support.

## References

- [1] Z. Aksu, Application of biosorption for the removal of organic pollutants: A review, *Process Biochem*, 40 (2005) 997–1026.
- [2] G.M. Walker, L. Hansen, J.A.Hanna, S.J. Allen, Kinetics of a reactive dye adsorption onto dolomitic sorbents, *Water Res*, 37(2003) 2081–2089.
- [3] M. Dogan, M. Alkan, Adsorption kinetics of methyl violet onto perlite, *Chemosphere*, 50 (2003) 517–528.
- [4] D. Inthorn, S. Singhtho, P. Thiravetyan, E. Khan, Decolorization of basic, direct and reactive dyes by pre-treated narrow-leaved cattail (*Typha angustifolia* Linn.), *Bioresour Technol*, 94 (2004) 299–306.
- [5] W.T. Tsai, C.Y. Chang, M.C. Lin, S.F. Chien, H.F. Sun, M.F. Hsieh, Adsorption of acid dye onto activated carbons prepared from agricultural waste bagasse by ZnCl<sub>2</sub> activation, *Chemospher*, 45 (2001) 51–58.
- [6] G. Mezohegyi, A. Kolodkin, U.I. Castro, C. Bengoa, F. Stuber, J. Font, A. Fabregat, A. Fortuny, Effective anaerobic decolorization of azo dye acid orange 7 in continuous upflowpacked-bed reactor using biological activated carbon system, *Ind. Eng. Chem. Res.*, 46 (2007) 6788–6792.
- [7] N. Dizge, C. Aydiner, E. Demirbas, M. Kobya, S. Kara, Adsorption of reactive dyes from aqueous solutions by fly ash: Kinetic and equilibrium studies, *J. Hazard Mater.*, 150 (2008) 737–746.
- [8] V.K. Garg, R. Gupta, A. Yadav, K. Kumar, Dye removal from aqueous solution by adsorption on treated sawdust, *Bioresour Technol*, 89 (2003) 121–124.
- [9] H. Tayebi, Z. Dalirandeh, A. Shokuhi-Rad, A. Mirabi, E. Binaian, Synthesis of polyaniline/Fe<sub>3</sub>O<sub>4</sub> magnetic nanoparticles for removal of reactive red 198 from textile waste water: kinetic, isotherm and thermodynamic studies, *Desalin Water Treat*, 57 (2016) 22551-22563.
- [10] K. Kadirvelu, M. Palanival, R. Kalpana, S. Rajeswari, Activated carbon from an agricultural by-product, for the treatment of dyeing industry wastewater, *Bioresour Techno*, 74 (2000) 263–265.
- [11] V.K. Gupta, A. Mittal, L. Krishnan, V. Gajbe, Adsorption kinetics and column operations for the removal and recovery of malachite green from wastewater using bottom ash, *Sep. Purif. Techno*, 40 (2004) 87–96.
- [12] A. Mittal, L. Kurup (Krishnan), V.K. Gupta, Use of waste materials Bottom Ash and De-Oiled Soya, as potential adsorbents for the removal of Amaranth from aqueous solutions. *J Hazard Mater*, 117 (2005) 171–178.
- [13] A. Mirabi, A. Shokuhi-Rad, F. Divsalar, H. Karimi-Maleh, Application of SBA-15/diphenyl carbazon/SDS nanocomposite as solid-phase extractor for simultaneous determination of Cu (II) and Zn (II) ions, *Arab J. Sci. Eng.*, 43 (2018) 3547-3556.
- [14] M.M. Sadeghi, A. Shokuhi-Rad, M. Ardjmand, A. Mirabi, Functionalization of SBA-15 by dithiooxamide towards removal of Co (II) ions from real samples: Isotherm, thermodynamic and kinetic studies, *Adv. Powder Technol*, 30 (2019) 1823–1834.
- [15] Z. Khanjari, A. Mirabi, A. Shokuhi-Rad, M. Moradian, . Selective removal of cadmium ions from water samples by using Br-PADAP functionalized SBA-15 particles, *Desalin Water Treat*, 130 (2018) 172-181.
- [16] A. Mirabi, S.N. Hossein, Use of modified nanosorbent materials for extraction and determination of trace amounts of copper ions in food and natural water samples, *Trends applied sci. res.*, 7 (2012) 541-549.
- [17] A. Shokuhi-Rad, A. Mirabi, M. Peyravi, M. Mirzaei, Nickel-decorated B<sub>12</sub>P<sub>12</sub> nanoclusters as a strong adsorbent for SO<sub>2</sub> adsorption: Quantum chemical calculations, *Can. J. Phys.*, 95 (2017) 958-962.
- [18] M. Sadeghi, M. Moradian, H.A. Tayebi, A. Mirabi, Removal of Penicillin G from Aqueous Medium by PPI@SBA-15/ZIF-8 Super Adsorbent: Adsorption Isotherm, Thermodynamic, and Kinetic Studies, *Chemosphere*, 311 (2023) 136887.
- [19] S. Kaveh, B. Norouzi, N. Nami, A. Mirabi, Phytochemical synthesis of CdO nanoparticles: fabrication of electrochemical sensor for quantification of cefixime, *J. Mater Sci.: Mater Electron*, 32 (2021) 8932–8943.
- [20] A. Mirabi, A. Shokuhi-Rad, M. Abdollahi, . Preparation of modified MWCNT with dithiooxamide for preconcentration and determination of trace amounts of cobalt ions in food and natural water samples, *Chemistry Select*, 2 (2017) 4439-4444.
- [21] Z. Aghaee-Meibodi, A. Mirabi, S. Khandan, B. Azizi, Fe<sub>3</sub>O<sub>4</sub>/CuO/ZnO@MWCNT MNCs Promoted the Green Synthesis of Indenopyrimidin-1,2,4-Triazoles as Hybrid Molecules, *Polycycl Aromat Compd.*, (2022) 1-24.
- [22] T. Pezeshkvar, B. Norouzi, M. Moradian, A. Mirabi, Fabrication of new nanocomposites based on NiO-MWCNT-sodium dodecyl sulfate in the presence of *Gundelia tournefortii* extract: application for methanol electrooxidation in alkaline solution, *J. Solid State Electrochem*, 26 (2022) 1479-1492.
- [23] A. Shokuhi-Rad, S. Bagheri-Novir, S. Mohseni, N. Ramezani-Cherati, A. Mirabi, A DFT study of O<sub>2</sub> and Cl<sub>2</sub> adsorption onto Al<sub>12</sub>N<sub>12</sub> fullerene-like nanocluster, *Heteroat Chem.*, 28 (2017) e21396.
- [24] S.A. Siadati, A. Mirabi, Diels-Alder versus 1,3-dipolar cycloaddition pathways in the reaction of C<sub>20</sub> fullerene and

- 2-furan nitrile oxide, *Prog. React. Kinet. Mech.*, 40 (2015) 383-390.
- [25] A. Mirabi, A. Shokuhi-Rad, M.R. Jamali, N. Danesh, Use of modified  $\gamma$ -alumina nanoparticles for the extraction and preconcentration of trace amounts of cadmium ions, *Aust. J. Chem.*, 69 (2015) 314-318.
- [26] S. Ahmadi-Asoori, A. Mirabi, E. Tazikeh-Lemseki, E. Babanezhad-Orimi, M. Habibi-Juybari, The Synthesis of Surfactant Coated Glass Foam to Extract and Determine Trace Quantities of Polycyclic Aromatic Hydrocarbons in Drinking Water, *J. Chem. Health Risks*, 11 (2021) 1-11.
- [27] A. Mirabi, Application of Modified Nanocellulose with 2-aminopyrimidine as a New Sorbent for Separation and Determination of Trace Amounts of Nickel Ions in Human Blood and Urine, *J. Chem. Health Risks*, 9 (2019) 35-50.
- [28] S. Movaghgharnezhad, A. Mirabi, M.R. Toosi, A. Shokuhi-Rad, Synthesis of cellulose nanofibers functionalized by dithiooxamide for preconcentration and determination of trace amounts of Cd (II) ions in water samples, *Cellulose*, 27 (2020) 8885-8898.
- [29] S. Ahmadi-Asoori, E. Tazikeh-Lemeski, A. Mirabi, E. Babanezhad, M. Habibi Juybari, Preparation of nanocellulose modified with dithizone for separation, extraction and determination of trace amounts of manganese ions in industrial wastewater samples, *Microchem J.*, 160 (2021) 105737.
- [30] S.S. Asadi-Ojaee, A. Mirabi, A. Shokuhi-Rad, S. Movaghgharnezhad, S. Hallajian, Removal of Bismuth (III) ions from water solution using a cellulose-based nanocomposite: A detailed study by DFT and experimental insights, *J. Mol. Liq.*, 295 (2019) 111723.
- [31] A. Mirabi-Semnokolaii, P. Daneshgar, A.A. Moosavi-Movahedi, M. Rezayat, P. Norouzi, A. Nemati, M. Farhadi, Sensitive determination of herbicide trifluralin on the surface of copper nanowire electrochemical sensor, *J. Solid State Electrochem.*, 15 (2011) 1953-1961.
- [32] S. Movaghgharnezhad, A. Mirabi, Advanced nanostructure amplified strategy for voltammetric determination of folic acid, *Int. J. Electrochem Sci.*, 14 (2019) 10956-10965.
- [33] T. Pezeshkvar, B. Norouzi, M. Moradian, A. Mirabi, Synthesis of nickel oxide nanostructures and its application for acyclovir antiviral drug sensing in the presence of sodium dodecyl sulfate, *Ionics*, 28 (2022) 4445-4459.
- [34] A. Mirabi, N. Aliakbari, Preparation of Modified Magnetic Nanocomposites Dithiooxamide/ $\text{Fe}_3\text{O}_4$  for Preconcentration and Determination of Trace Amounts of Cobalt Ions in Food and Natural Water Samples, *J. Chem. Health Risks*, 6(2016) 291-303.
- [35] A. Mirabi, A. Shokuhi-Rad, H. Khodadad, Modified surface based on magnetic nanocomposite of dithiooxamide / $\text{Fe}_3\text{O}_4$  as a sorbent for preconcentration and determination of trace amounts of copper, *J. Magn. Magn. Mater.*, 389 (2015) 130-135.
- [36] M.M. Sadeghi, A. Shokuhi-Rad, M. Ardjmand, A. Mirabi, Preparation of magnetic nanocomposite based on polyaniline/ $\text{Fe}_3\text{O}_4$  towards removal of lead (II) ions from real samples, *Synth. Met.*, 245 (2018) 1-9.
- [37] A. Mirabi, A. Shokuhi-Rad, S. Nourani, Application of Modified Magnetic Nanoparticles as a Sorbent for Preconcentration and Determination of Nickel Ions in Food and Environmental Water Samples, *Trends Anal Chem.*, 74 (2015) 146-151.
- [38] A. Mirabi, A. Shokuhi-Rad, S. Ahmadizadeh, Graphene oxide enhances SBA-15 ability towards preconcentration as well as determination of barbiturate drug in real samples, *Kuwait J. Sci.*, 46 (2019) 41-49.
- [39] A. Mirabi, A. Shokuhi-Rad, Z. Khanjari, M. Moradian, Preparation of SBA-15/graphene oxide nanocomposites for preconcentration and determination of trace amounts of rutoside in blood plasma and urine, *Sens Actuators B: Chem.*, 253 (2017) 533-541.
- [40] S. Kaveh, N. Nami, B. Norouzi, A. Mirabi, Biosynthesis of (MWCNTs)-COOH/CdO hybrid as an effective catalyst in the synthesis of pyrimidinethione derivatives by water lily flower extract, *Inorg Nano-Met Chem.*, 51 (2021) 1459-1470.
- [41] V.B. Cashin, D.S. Eldridge, A. Yu, D. Zhao, Surface functionalization and manipulation of mesoporous silica adsorbents for improved removal of pollutants: a review, *Environ Sci. Water Res. Technol.*, 4 (2018) 110-128.
- [42] Y. Zhu, Z. Cheng, Q. Xiang, J. Xu, Rational design and synthesis of aldehyde-functionalized mesoporous SBA-15 for high-performance ammonia sensor, *Sens Actuators B.*, 256 (2018) 888-895.
- [43] I. Yuranov, L. Kiwi-Minsker, P. Buffat, A. Renken, Selective synthesis of Pd nanoparticles in complementary micropores of SBA-15, *Chem. Mater.*, 16 (2004) 760-761.
- [44] A.Y. Khodakov, V.L. Zholobenko, R. Bechara, D. Durand, Impact of aqueous impregnation on the long-range ordering and mesoporous structure of cobalt containing MCM-41 and SBA-15 materials, *Micropor Mesopor Mat.*, 79 (2005) 29-39.
- [45] S.G. de-Avila, L.C.C. Silva, J.R. Matos, Optimisation of SBA-15 properties using Soxhlet solvent extraction for template removal, *Micropor Mesopor Mat.*, 234 (2016) 277-286.
- [46] Y. Yamini, J. Hassan, R. Mohandesi, N. Bahramifar, Preconcentration of trace amounts of beryllium in water

- samples on octadecyl silica cartridges modified by quinalizarine and its determination with atomic absorption spectrometry, *Talanta*, 56(2002) 375–381.
- [47] V.K. Gupta, P. Singh, N. Rahman, Adsorption behavior of Hg(II), Pb(II), and Cd(II) from aqueous solution on Duolite C-433: a synthetic resin, *J. Colloid Interf. Sci.*, 275(2004) 398–402.
- [48] A.A. Atia, A.M. Donia, K.Z. Elwakeel, Adsorption behaviour of non-transition metal ions on a synthetic chelating resin bearing iminoacetate functions, *Sep. Purif. Technol.*, 43(2005) 43–48.
- [49] A. Demirbas, E. Pehlivan, F. Gode, T. Altun, G. Arslan, Adsorption of Cu(II), Zn(II), Ni(II), Pb(II), and Cd(II) from aqueous solution on Amberlite IR-120 synthetic resin, *J. Colloid Interf. Sci.*, 282 (2005) 20–25.
- [50] V.D. Grebenyuk, S.V. Verbich, N.A. Linkov, V.M. Linkov, Adsorption of heavy metal ions by aminocarboxyl ion exchanger ANKB-35, *Desalination*, 115 (1998) 239–254.
- [51] F. Sheikholeslami-Farahani, S. Sadeghi-Marasht, A. Mirabi, M. Ghazvini, M. Hosseinnasab-Rostam, Ionic Liquid as Green and Recyclable Solvent for the Synthesis of Pyrazinoquinazolines: Study of Antioxidant Activity, *Polycycl Aromat Compd.*, 42 (2022) 3663–3674.
- [52] A. Mirabi, M.R. Jamali, Q. Kazemi, Determination of trace amounts of manganese in water samples by flame atomic absorption spectrometry after dispersive liquid-liquid microextraction, *Bulg. Chem. Commun*, 48 (2016) 525–531.
- [53] B. Salih, A. Denizli, C. Kavakli, R. Say, E. Piskin, . Adsorption of heavy metal ions onto dithizone-anchored poly (EGDMAHEMA) microbeads, *Talanta*, 46 (1998) 1205–1213.
- [54] A.A. Atia, A.M. Donia, A.M. Yousif, Synthesis of amine and thio chelating resins and study of their interaction with zinc (II), cadmium (II) and mercury (II) ions in their aqueous solutions, *React. Funct. Polym.*, 56 (2003) 75–82.